# UNIVERSITYOF BIRMINGHAM

University of Birmingham
Research at Birmingham

# Tumor-derived TGF- inhibits mitochondrial respiration to suppress IFN- production by human CD4+ T cells

Dimeloe, Sarah; Gubser, P; Loeliger, J; Frick, C; Develioglu, Leyla; Fischer, M; Marquardsen, F; Bantug, Glenn R; Thommen, Daniela S; Lecoultre, Y; Zippelius, Alfred; Langenkamp, A; Hess, Christoph

Link to publication on Research at Birmingham portal

**Tumor-derived TGF-β inhibits mitochondrial respiration to suppress IFN-γ production by human CD4^{+} T cells**

**One sentence summary:**

TGF-β in human malignant effusions inhibits CD4^{+} T cell production of IFN-γ, a key anti-tumor cytokine, by inhibition of mitochondrial complex V and suppression of cellular ATP-coupled respiration.

Sarah Dimeloe[1,2,*], Patrick Gubser[1]*, Jordan Loeliger[1], Corina Frick[1], Leyla Develioglu[1], Marco Fischer[1], Florian Marquardsen[3], Glenn R. Bantug[1], Daniela Thommen[4], Yannic Lecoultre[1], Alfred Zippelius[4], Anja Langenkamp[5] and Christoph Hess[1,6]

[1] Immunobiology Laboratory, Department of Biomedicine, University of Basel, 4031 Basel, Switzerland

[2] Institute of Immunology and Immunotherapy, Institute of Metabolism and Systems Research, University of Birmingham, Birmingham B15 2TT, UK

[3] Immunodeficiency Laboratory, Department of Biomedicine, University of Basel, 4031 Basel, Switzerland

[4] Cancer Immunology Laboratory, Department of Biomedicine, University of Basel, 4031 Basel, Switzerland

[5] Roche Innovation Center Basel, 4070 Basel, Switzerland

[6] Department of Medicine, University of Cambridge, Cambridge CB2 0QQ, UK

* Equal contribution

**Abstract**

TGF-β is produced by tumors, and increased levels are associated with poor survival. Functionally, TGF-β-mediated suppression of anti-tumor T cell responses contributes to tumor growth and survival. However, TGF-β can also have tumor suppressive activity, and dissecting cell-type specific molecular effects may decisively inform therapeutic strategies targeting this cytokine. Here we investigated the mechanisms involved in suppression of a key anti-tumor CD4^{+} T cell function – interferon-γ (IFN-γ) production– by tumor-derived TGF-β in human peripheral and tumor-associated lymphocytes. Suppression required expression and phosphorylation of TGF-β signaling proteins (Smad proteins), but not their nuclear translocation, and was dependent on oxygen availability – suggesting a metabolic basis. Indeed, Smad proteins were detected in mitochondria of CD4^{+} T cells, where they were phosphorylated upon TGF-β exposure. Phosphorylated Smad proteins were also detected ex vivo in mitochondria of tumor-associated lymphocytes. TGF-β treatment significantly impaired ATP-coupled respiration of CD4^{+} T cells, and specifically mitochondrial complex V (ATP-Synthase) activity. Finally, inhibition of ATP-Synthase *per se* was sufficient to impair IFN-γ production. These results demonstrate that TGF-β targets T cell metabolism directly, thus diminishing their function (metabolic paralysis), with relevance to human anti-tumor immunity.

**Introduction**

Transforming growth factor β1 (TGF-β) plays a complex role in tumor initiation and progression, demonstrating both tumor-suppressive and tumor-promoting activities. Tumor-suppressive activities of TGF-β are linked to its capacity to inhibit cellular proliferation, induce apoptosis and suppress growth factor expression (1). However, many tumor types produce TGF-β in large quantities, and this is associated with metastasis and poor patient prognosis. Tumor-promoting activities of TGF-β include dysregulation of the cell cycle, increased extracellular matrix formation, angiogenesis and, importantly, inhibition of anti-tumor T cell immunity (1).

A critical immune-regulatory role for TGF-β was established by the lethal inflammatory phenotype of TGF-β deficient mice (2). T cells are critical targets of TGF-β, as specific deletion of the TGF-βRII on T cells phenocopied this disease (3, 4). Indeed, TGF-β influences thymic selection and differentiation of mature T cells to promote central and peripheral immune tolerance (5-7). TGF-β inhibits T cell proliferation and suppresses differentiation and function of cytotoxic CD8^{+} T cells, as well as pro-inflammatory "T helper" (Th)1 and Th2 CD4^{+} T cell subsets. Conversely, TGF-β promotes expression of the transcription factor FoxP3, driving regulatory T cell (TReg) development. However, reconstitution of TRegs could only partially rescue disease in T cell TGF-βRII deficient mice (4, 5), indicating the significance of direct T cell inhibitory activities of TGF-β.

Because of its tumor-promoting and immune-regulatory roles, TGF-β may present a valuable therapeutic target in cancer. Indeed, small molecule inhibitors of TGF-β receptor signaling, TGF-β-neutralizing antibodies and oligonucleotides targeting TGF-β are currently under investigation in clinical trials (8). However, completely inhibiting TGF-β activity may also impair its beneficial

tumor-suppressive activity. A deeper understanding of TGF-β signaling and cellular effects is therefore required to inform precise and context-appropriate therapeutic approaches.

TGF-β binds its tetrameric receptor complex of TGF-βRI and TGF-βRII to trigger receptor serine/threonine kinase activity and phosphorylation of downstream targets. In the canonical model of TGF-β signaling, phosphorylated Smad2 and Smad3 interact with Smad4. Subsequent nuclear translocation of this trimeric complex leads to transcriptional gene regulation (9). Smad-independent TGF-β signaling pathways are also described, involving PI(3)-kinase, p38 kinase and small GTPases such as RhoA and Rock (1), and recently a TGF-β-independent role for Smad4 in T cells was identified (10). In addition to transcriptional regulation, direct interaction of Smads with other proteins has also been identified (11). These include p53/p63 complexes, inhibiting their tumor-suppressive function (1), as well as subunits of the mitochondrial electron transport chain (ETC), which was reported to increase ROS production and promote apoptosis (12). Here we assessed the impact of tumor-derived TGF-β on human CD4$^+$ T cell effector function and identified TGF-β mediated cellular mechanisms which may inform targeted therapeutic interventions to rescue suppression of anti-tumor immunity by TGF-β.

**Results**

The tumor microenvironment can be rich in TGF-β, which is implicated in preventing effective anti-tumor T cell responses. We quantified TGF-β in a panel of eleven effusion fluids from a range of human metastatic tumors (**Tbl. 1**, **Fig. 1A**) and assessed their effect on production of interferon (IFN)-γ by effector memory (EM) CD4$^+$ T cells, which comprise the majority of tumor-infiltrating CD4$^+$ T lymphocytes (13). Specifically, activated human EM (CD127$^+$CD25$^-$CD45RA$^-$ CCR7$^-$) CD4$^+$ T cells from healthy donors were stimulated for 16 hours in the presence of tumor effusion fluid (50% with 50% serum-free medium to buffer pH), and additionally either an isotype control antibody or a specific antibody to neutralize TGF-β. These assays identified that neutralization of TGF-β in effusion fluids increased the frequency of EM CD4$^+$ T cells expressing IFN-γ, with a strong positive correlation between the concentration of TGF-β in the respective effusions and the capacity to rescue IFN-γ production by blocking this cytokine (**Fig. 1B**). TGF-β is reported to signal by both canonical pathways involving Smad phosphorylation, nuclear translocation and transcriptional regulation, as well as non-canonical Smad-dependent and -independent pathways (1, 9). Understanding the relative importance of the respective signaling mechanisms in driving a given outcome should inform therapeutic strategies that aim at targeting TGF-β signaling to restore T cell function. To investigate the cellular mechanisms involved in TGF-β-mediated suppression of IFN-γ, effusion fluids with TGF-β-dependent inhibitory capacity (n=8) were further characterized. The effect of neutralizing TGF-β in these effusions on the frequency of IFN-γ-producing cells, and on total IFN-γ secreted into the supernatant, is shown in **Figure 1C**-**F**. We then interrogated the requirement for Smad phosphorylation and nuclear translocation in our system, using pharmacological inhibitors –namely the activin receptor-like kinase (ALK) inhibitor SB-431542,

which prevents Smad phosphorylation (14), and ivermectin, which inhibits the importin α/β nuclear transporters involved in Smad nuclear translocation (Refs. 15, 16, and **Suppl. Fig 1**). These experiments showed that suppression of IFN-γ production by tumor effusions was abrogated by inhibition of Smad phosphorylation, but, conversely, was unaffected by inhibiting nuclear Smad import with ivermectin (**Fig. 1G**-**H**). Thus, Smad phosphorylation, but not nuclear translocation, was required for the immune-suppressive effect of tumor-derived TGF-β on EM CD4$^+$ T cells. Inhibition of IFN-γ expression was also not observed under hypoxic conditions (**Fig. 1I**-**J**), a hint that the observed nuclear translocation-*independent* mechanism may have a metabolic basis.

To directly investigate whether TGF-β affects the metabolism of CD4$^+$ T cells, we next exposed activated EM CD4$^+$ T cells to TGF-β for 16 hours and then measured their respiratory and glycolytic capacity (for a detailed explanation of metabolic parameters refer to **Suppl. Fig. 2A**-**D**). This revealed that treatment with TGF-β resulted in significantly decreased basal and ATP-coupled oxygen consumption rates (OCR) (by approximately 30 and 40% respectively), with no change in spare respiratory capacity (SRC) (**Fig. 2A**-**D**). Comparison of ATP-coupled vs. FCCP-stimulated maximal OCR identified that the TGF-β mediated suppression of ATP-coupled OCR was partially rescued by FCCP treatment (with 40% suppression decreasing to ~20%), implying that a functional inhibition of the electron transport chain (ETC) may be at least partly responsible. A modest, yet consistent, decrease of basal and maximal rates of glycolysis was also observed (**Fig. 2F**-**H**). The impact of TGF-β on mitochondrial respiration was, however, greater than that on glycolysis, as evidenced by a decreased OCR/ECAR ratio (**Fig. 2I**). Of note, inhibition of basal and ATP-coupled OCR by TGF-β was unhindered in the presence of ivermectin, but did not occur when treating cells with SB-431542 – indicating that Smad phosphorylation, but not nuclear translocation, was required also for these metabolic effects (**Suppl. Fig 3A**-**B**). The role of Smad2 in TGF-β-mediated metabolic

suppression was further confirmed by genetic manipulation of its expression. Smad2 protein abundance was efficiently reduced in primary CD4^{+} T cells and Jurkat T cells (by approx. 75% and 60% respectively – **Suppl. Fig 4**) by transfection with siRNA. Subsequent metabolic analyses of these cells revealed that TGF-β exposure of cells treated with Smad2 siRNA achieved significantly less suppression of ATP-coupled respiration than in cells treated with control siRNA. Again glycolysis was only modestly affected, with no significant difference between control- and Smad2-siRNA treated cells (**Figure 2J**-**K**). TGF-β did not impact the viability of activated EM CD4^{+} T cells at this time point (**Fig. 2L**).

Activation of naïve murine CD4^{+} T cells in the presence of TGF-β for prolonged periods of time –to induce differentiation of regulatory T cells (TReg)– has been reported to increase, rather than decrease, mitochondrial respiratory capacity, further associated with increased fatty acid oxidation (FAO) (17). Indeed, and contrary to the reduction in ATP-coupled respiration observed when treating activated EM CD4^{+} T cells with TGF-β for only 16 hours (**Fig. 2**), we also observed that anti-CD3/anti-CD28 mAb mediated activation of bulk human CD4^{+} T cells for 72 hours in the presence of 2 ng/ml of TGF-β (which increased the frequency of FoxP3^{+} TReg (**Suppl. Fig. 5A**)), increased mitochondrial membrane potential (ΔΨm) and SRC (**Suppl. Fig. 5B**-**D**). Rates of glycolysis were not influenced by activation of CD4^{+} T cells in the presence of TGF-β (**Suppl. Fig. 5E**,**F**). TGF-β thus differentially impacted mitochondrial function depending on the duration of exposure.

One mechanism by which TGF-β may inhibit CD4^{+} T cell ATP-coupled respiration is modulation of the activity of mechanistic target of rapamycin (mTOR) complex 1 (mTORC1), a master regulator of cellular metabolism. To interrogate this, we first assessed mTORC1 activity by studying phosphorylation of a key target protein, p70S6 kinase (p70S6K). These experiments

revealed that TGF-β treatment of activated total CD4$^+$ T cells did significantly suppress mTORC1 activity, which was dependent upon Smad2 phosphorylation (**Suppl. Fig 6A**-**B**). Therefore, we next interrogated the extent to which mTORC1 inhibition was responsible for the observed effects of TGF-β on CD4$^+$ T cell metabolism, by comparison with the mTORC1 inhibitor rapamycin. These assays identified that both TGF-β and rapamycin significantly reduced ATP-coupled oxygen consumption of activated CD4$^+$ T cells, and furthermore that there was an additive effect in cells treated with both compounds – indicating mTORC1-*independent* effects of TGF-β on mitochondrial function (**Suppl. Fig 6C**-**D**), in agreement with the data in **Fig. 2E,** which suggested a functional ETC inhibition. Effects of rapamycin and TGF-β on glycolysis were again more modest and furthermore there was no additive effect of both compounds (**Suppl. Fig 6C-D**).

To further dissect these mTORC1-independent effects, we first investigated whether TGF-β treatment impacted the transcription of a panel of master regulators of mitochondrial biogenesis. Following 5 or 24 hours of treatment with TGF-β, mRNA levels of these gene products in total, activated CD4$^+$ T cells were unaffected (**Fig. 3A**). Consistent with this, exposure to TGF-β for 24 hours also did not affect overall expression levels of ETC complexes I-V (**Fig. 3B**). These data therefore also pointed to a potential direct inhibition of mitochondrial function, rather than a transcriptional regulation of mitochondrial component expression. Based on their structure, TGF-β signaling proteins (Smad 2, 3 and 4) are predicted to localize to mitochondria (18) and have been detected in mitochondrial fractions of non-lymphoid cells (12). We therefore examined subcellular localization of pSmad2/3 by imaging flow cytometry (**Fig. 3C**). CD4$^+$ T cells were, in addition to pSmad2/3, stained with mitotracker red (MTR) and 4,6-diamidino-2-phenylindole (DAPI) to identify mitochondria and nuclei, respectively. Analysis of fluorochrome abundance in these cellular compartments confirmed a significant enrichment of MTR in mitochondria compared to the nuclear

marker DAPI, and furthermore identified that pSmad2/3 was enriched in mitochondria compared to DAPI (**Fig. 3D**). Comparison of control and TGF-β treated cells revealed increased abundance of pSmad2/3 upon TGF-β treatment in both nuclear and mitochondrial compartments, which was comparable in terms of fold increase (**Fig. 3E,F**). These data indicated that phosphorylated Smad proteins were present in mitochondria of CD4^{+} T cells, and phosphorylation was increased upon TGF-β treatment. Evidence for in vivo relevance of mitochondrial pSmad2/3 was obtained by studying tumor-associated CD4^{+} T cells (recovered from the effusion fluids utilized above). Direct ex vivo staining of pSmad2/3 in these cells, and analysis by flow cytometry, revealed that abundance of pSmad2/3 in tumor-associated CD4^{+} T cells closely reflected the TGF-β concentration of the respective effusion fluid from which the cells were recovered (**Fig. 3G/Fig.1A, Tbl. 1**). Additionally, imaging analysis identified a similar enrichment of pSmad2/3 in mitochondria of tumor-associated CD4^{+} T cells compared to DAPI, as was observed for peripheral counterparts in vitro (**Fig. 3H,I**).

To define the molecular basis through which mitochondrial Smad proteins impacted CD4^{+} T cell respiration, we assessed what aspect of mitochondrial function was impaired. The function of ETC complexes I, II, III and IV was assessed by measuring oxygen consumption rates of isolated mitochondria in response to the provision of specific substrates or electron donors for each complex (**Suppl. Fig. 7A**-**D**). Performing such analyses on mitochondria isolated from activated EM CD4^{+} T cells pre-cultured for 5 hours in control or TGF-β containing medium demonstrated decreased oxygen consumption in response to all four substrates/electron donors (**Fig. 4A**, **Suppl. Fig. 7A**-**D**). This implied either (i) decreased functionality of all ETC complexes, (ii) decreased function of complex IV (which consumes the oxygen that is measured), or (iii) decreased function of complex V, ATP-Synthase, which may subsequently impact efficiency of the entire ETC – and cannot be directly measured in these experiments. To answer this question we next undertook biochemical studies

selectively measuring activity of complex I, II, IV or V, using cell lysates of control and TGF-β treated, activated total CD4^{+} T cells. In TGF-β treated cells, these assays revealed no inhibition of the function of complexes I, II and IV, but significant inhibition of complex V activity (**Fig. 4B**). Consistent with an inhibition of complex V activity, TGF-β treatment also caused a significant increase in T cell mitochondrial membrane potential (**Fig. 4C**).

Both glycolytic and mitochondrial functionality of T cells critically underpin key immune functions (19). We next probed the impact of metabolic inhibition by TGF-β on the immune function of EM CD4^{+} T cells – specifically on IFN-γ production, which we had observed to be significantly impaired by TGF-β present in tumor effusions (**Fig. 1**). Indeed, performing multiplex cytokine analyses we confirmed that TGF-β treatment most profoundly inhibited secretion of IFN-γ in EM CD4^{+} T cells, compared to other cytokines (interleukin (IL)-10, IL-17) (**Fig. 5A**). Inhibition of IFN-γ secretion by TGF-β in other subsets of activated CD4^{+} T cells (naïve and central memory) was less marked and did not reach statistical significance (**Suppl. Fig 8A**), which was consistent with lower expression of TGF-βRII and less TGF-β-induced Smad2/3 phosphorylation in these cells (**Suppl. Fig 8B-E**). TGF-β can inhibit IFN-γ expression by transcriptional repression of the *TBX21* (T-bet) and *IFNG* (IFN-γ) genes (9, 20). However, we observed that nuclear translocation was not required for TGF-β dependent inhibition of IFN-γ expression by tumor effusions (**Fig. 1**). To further define TGF-β mediated transcriptional vs. metabolic regulation of IFN-γ production, we again blocked nuclear import of Smad proteins using the nuclear import inhibitor, ivermectin, and compared its effects to inhibition of Smad phosphorylation with SB-431542. We first confirmed, by flow cytometric analysis of pSmad2/3 abundance, that treatment with SB-431542 – *but not* ivermectin – prevented TGF-β mediated phosphorylation of Smad2/3 (**Fig. 5B**). Next, having verified by imaging flow cytometry

and imaging that ivermectin and SB-431542 both inhibited nuclear pSmad2/3 import (**Fig. 5C, Suppl. Fig. 1**), we furthermore confirmed that both inhibitors prevented transcriptional repression of T-bet (TBX21), and IFN-γ (IFNG) (**Fig. 5D**). We then assessed IFN-γ production and observed that TGF-β treatment still inhibited IFN-γ production even in the presence of ivermectin, which blocked nuclear import of phosphorylated Smad proteins and thus transcriptional effects of TGF-β. However, inhibiting Smad phosphorylation with SB-431542 abolished the inhibitory effects of TGF-β on IFN-γ production (**Fig. 5E**), indicating critical roles for phosphorylated Smad proteins in inhibiting IFN-γ production by EM CD4$^+$ T cell, by transcription-independent mechanisms. These experiments therefore concur with our initial observations using tumor effusions. We then aimed to verify the relevance of TGF-β-mediated suppression of IFN-γ in tumor-associated T cells. To do so, we assessed IFN-γ production by tumor-associated T cells (n=3 independent donors), activated in presence of TGF-β at the concentration that was present in their respective effusion fluids, plus either an isotype control or TGF-β-neutralizing mAb (to inactivate any TGF-β produced by tumor cells in the culture). Aligning with the in vitro functional and mechanistic experiments, these assays confirmed that effusion-level TGF-β also inhibited tumor-associated T cells directly ex vivo, compared to cultures treated with TGF-β neutralization, with a magnitude that reflected the respective effusion TGF-β concentration (**Fig. 5F left panel/Fig. 1A, Tbl. 1**). Furthermore, in two donors where sufficient cells were available, we additionally observed that TGF-β-mediated IFN-γ suppression occurred despite blockade of Smad nuclear import with ivermectin (**Fig. 5F right panel**).

Next, we assessed whether inhibition of complex V and other ETC complexes *per se* could impact IFN-γ production by EM CD4$^+$ T cells, by treating cells with specific inhibitors. Indeed, complex V inhibition with oligomycin was sufficient to decrease both the percentage of EM CD4$^+$ T

cells producing IFN-γ, as well as the total amount of IFN-γ secreted by these cells (**Fig. 5G,H**), which was also true for inhibition of complexes I, II III and IV (**Suppl. Fig. 9A-D**). Unhindered mitochondrial ETC function was thus required for IFN-γ production by EM CD4⁺ T cells, and seems to be specifically targeted –at the level of complex V– by TGF-β signaling. Notably, oligomycin treatment did not achieve the same degree of IFN-γ suppression TGF-β treatment – indicating that TGF-β acts by additional pathways in the cytoplasm to suppress IFN-γ production (for example inhibition of mTORC1). However, when cells were treated with TGF-β, no additional suppression of IFN-γ could be achieved by adding in oligomycin, suggesting the ETC-linked IFN-γ was already maximally suppressed by TGF-β treatment (**Fig. 5I**). Further confirmation that inhibition of mitochondrial function played an important role in the suppression of IFN-γ production by TGF-β in EM CD4⁺ T cells, came from observations that IFN-γ expression was not inhibited by TGF-β under hypoxic conditions, which was also true for the complex V inhibitor, oligomycin (**Fig. 5J-K**), and for the tumor effusions (**Fig. 1I-J**).

To assess whether direct metabolic inhibition, driven by TGF-β, was recapitulated using clinical samples rich in this cytokine, we assessed the capacity of two tumor effusions – described in **Supplementary Table 1/Figure 1** – to impact metabolic parameters of activated EM CD4⁺ T cells. These assays confirmed that activated EM cells, cultured in the presence of effusion fluid with an isotype control antibody, had reduced ATP-coupled respiration compared to cells cultured identically, yet in the presence of a specific mAb to neutralize TGF-β (**Fig. 6A,B**). Basal rates of glycolysis were also slightly reduced in these cells, yet calculation of OCR/ECAR ratios again indicated the effect on respiration to be greater (**Fig. 6C**).

**Discussion**

Production of TGF-β by tumors is associated with metastasis and poor patient prognosis. This is related to both tumor-promoting and immune-inhibitory effects of TGF-β, but tumor-suppressive activities of TGF-β are also described (1). Thus, while TGF-β is a promising therapeutic target for cancer, fully exploiting its potential will require a precise and context-specific understanding of its cellular effects.

Here we investigated the cellular mechanisms involved in TGF-β mediated inhibition of an important CD4^{+} T cell anti-tumor function, IFN-γ production (21). We found that effusions from metastatic human tumors impaired IFN-γ production in a TGF-β-dependent manner, and furthermore that TGF-β used at concentrations observed ex vivo suppressed IFN-γ production of human tumor-associated T cells. This immune-suppression occurred by a mechanism requiring phosphorylation of the Smad signaling proteins, but, surprisingly, not their nuclear translocation. Rather, inhibition was dependent on environmental oxygen abundance and indeed we identified that Smad proteins were present and phosphorylated within mitochondria of T cells exposed to TGF-β both in vitro and in vivo and that TGF-β treatment significantly impaired both complex V activity and ATP-coupled respiration –the latter in a *Smad2 dependent* manner. Additionally, complex V inhibition *per se* was sufficient to impair IFN-γ production by CD4^{+} T cells.

TGF-β signaling has previously been reported to impact metabolism at both the organismal and cellular level. Increased hypothalamic TGF-β in obesity and aging has been linked to systemic glucose intolerance (22). More directly, mice deficient in Smad3 or treated with TGF-β neutralizing antibodies were protected from diet-induced obesity and diabetes, which was associated with

13

'browning' of white adipocytes, heightened mitochondrial biogenesis and augmented respiratory capacity of these cells (23). We found no transcriptional regulation of a panel of transcription factors orchestrating mitochondrial biogenesis after 5 and 24 hours of treatment with TGF-β. However, activation of total CD4$^+$ T cells for 72 hours in presence of TGF-β, to promote TReg differentiation, did increase mitochondrial respiratory capacity and FAO –consistent with previous reports (17)– indicating duration-dependent effects of TGF-β on CD4$^+$ T cells. At the cellular level, TGF-β itself has previously been detected in the mitochondria of cardiomyocytes, hepatocytes and T cells (24-26). T cells lacking TGF-β have abnormal mitochondrial morphology, indicating a possible homeostatic role for TGF-β in mitochondrial biogenesis and/or dynamics (26). To date, cell-intrinsic vs. autocrine signaling-dependent effects of TGF-β have, however, not been assessed. Functionally, TGF-β exposure has been reported to decrease mitochondrial membrane potential in human fibroblasts (27), electron transport chain (ETC) complex IV activity in murine lung epithelial cells (28, 29), and function of complex IV in murine renal podocytes (30). TGF-β also regulates cellular metabolism through effects on mTOR complex I (mTORC1) activity. We confirmed inhibition of mTORC1 in human CD4$^+$ T cells by TGF-β, and furthermore that direct mTORC1 inactivation significantly repressed CD4$^+$ T cell respiration. However we additionally showed –by combining TGF-β treatment with direct mTORC1 inhibition– that TGF-β has significant effects on CD4$^+$ T cell mitochondrial respiration *independent* of mTORC1 regulation. TGF-β was also reported to impair mitochondrial calcium uptake in renal arteriolar cells (31). Since calcium flux is critical for T cell signaling, this observation is of particular interest. Smad signaling proteins, based on their structure, are predicted to localize to mitochondria (18), and indeed Smad 3, 4 and 5 have been detected in mitochondria of various cell types –not including immune cells (12, 18). Our study now links complex V-associated

Smad and TGF-β driven phosphorylation thereof, with mitochondrial suppression and impaired immune functionality.

Activation of T cells drives important changes in cellular metabolism which are critical for their effector function, through bioenergetic and non-bioenergetic mechanisms (32, 33). The signaling pathways that drive metabolic reprograming during T cell activation are quite well characterized and involve the PI(3)-kinase–Akt–mTOR axis, as well as the transcription factors c-Myc, estrogen-related receptor α (ERR-α) and AP4 (19). Signaling from inhibitory receptors, such as CTLA-4 and PD-1, antagonizes these pathways to limit metabolic reprogramming (34). T cell effector function is also limited in the tumor microenvironment by competition for metabolic precursors (35, 36). To date, cell extrinsic signals that directly modulate T cell metabolism to mediate an immune-regulatory effect have not been described. For TGF-β, such a role is consistent with both its immune-regulatory function and its abundance in malignantly transformed tissue sites. Selectively alleviating T cell metabolic paralysis induced by TGF-β, while maintaining transcriptional activity with postulated anti-tumor activity, might prove to be an effective strategy for cancer therapy.

**Materials and Methods**

**Study Design**

The objective of this research was to investigate the mechanism by which human tumor-derived TGF-β suppresses the immune function of human CD4$^+$ T cells. This research was carried out using biological material (tumor effusions and T cells) from cancer patients, and T cells isolated from peripheral blood of healthy donors. The experimental design consisted of controlled laboratory in vitro studies and ex vivo analyses of patient cells as described below. No data were excluded from analyses. Experiments were performed at least three times using cells from independent human donors. Exact numbers of replicates are stated in the figure legends (n=x).

**Peripheral blood CD4$^+$ T cell isolation, sorting and culture**

Bulk CD4$^+$ T cells were isolated as described previously (37). Where indicated, flow cytometry-sorted cell populations were used. T cell populations were sorted according to the expression of CD127, CD25, CD45RA and CCR7 to purify effector memory (EM) cells (CD127$^+$CD25$^-$CD45RA$^-$CCR7$^-$). Purity was typically >90%. The following mAb were used: anti-CD45RA mAb–Pacific Blue (clone 2H4; Beckman Coulter, Brea, CA), anti-CD25 mAb–Brilliant Violet 605 (clone 2A3; BD Biosciences, Mountain View, CA), anti-CCR7 mAb–PE (clone FABP197; R&D Systems Europe, Abingdon, U.K.), and anti-CD127 mAb–allophycocyanin (clone eBioRDR5; eBioscience, San Diego, CA). Cells were (unless otherwise indicated) resuspended at 1 x 10$^6$/ml in RPMI1640 containing 10% AB$^+$ human serum, 50 U/ml penicillin and 50 mg/ml streptomycin (Invitrogen, Carlsbad, CA) (RPMI/10%AB), and 50 IU/ml rIL-2 (PeproTech, Rocky Hill, NJ). Where serum-free medium is indicated, AIM-V serum-free medium (Invitrogen) containing 50 IU/ml rIL-2 was used. Cells were activated where indicated by placing in cell culture plates pre-coated with anti-CD3 and anti-CD28 (1 μg/ml and 5 μg/ml, clones OKT-3 and CD28.2 respectively, Biolegend, London, U.K.)

16

for 72 hours. Activated cells were then washed and resuspended at $1 \times 10^6$/ml in RPMI/10%AB or AIM-V medium (as indicated) under experimental conditions described in the figure legend.Additions to cell culture included: TGF-$\beta$ (2-20 ng/ml) (Peprotech, Rocky Hill, NJ), Ivermectin (5 $\mu$M, Sigma-Aldrich, Schnelldorf, Germany), SB-431542 (10 $\mu$M, SelleckChem, Luzern, CH), Rapamycin (20ng/ml, (Merck), Oligomycin (1 $\mu$M, Sigma-Aldrich), Rotenone (0.1 $\mu$M, Sigma-Aldrich), 2-thenoyltrifluoroacetone (TTFA) (200 $\mu$M, Sigma-Aldrich), Antimycin A (2 $\mu$M, Sigma-Aldrich), Sodium Azide (10 $\mu$M, Sigma-Aldrich), mouse IgG1 isotype control antibody (5 $\mu$g/ml, clone 11711 R&D Systems Europe), anti-TGF-$\beta$ mouse IgG1 monoclonal antibody (5 $\mu$g/ml, clone 1D11, R&D Systems Europe).

**Tumor effusion samples**

Tumor effusion fluids were collected from cancer patients presenting with malignant effusions at the University Hospital Basel after obtaining written informed consent. After collection, the cellular components of the malignant effusions were separated by centrifugation and cells and fluids were frozen at -80°C until further use. Where indicated, total effusion cells were cultured or analyzed, and CD4$^+$ T cells identified by staining with CD4-FITC (clone RPA-T4, BD Biosciences). Patient details are provided in **Supplementary Table 1**.

**RNA-mediated interference**

Activated primary human CD4$^+$ T cells or Jurkat cells were transfected with pools of Smad2-specific siRNA or control scrambled siRNA (QIAGEN) for 72 hours using the AMAXA T cell nucleofection kit (Lonza). Knockdown efficiency was verified by Western blotting analysis.

**Extracellular metabolic flux analysis of intact cells and isolated mitochondria**

For analysis of the OCR (in pmol/min) and ECAR (in mpH/min), the Seahorse XF$^e$96 metabolic extracellular flux analyzer was used (Seahorse Bioscience). Total or sorted CD4$^+$ T cells were

resuspended in serum-free, unbuffered RPMI 1640 medium (Sigma-Aldrich) and were plated onto Seahorse cell plates ($2.5 \times 10^5$ cells per well) coated with Cell-Tak (BD Biosciences) to enhance T cell attachment. Perturbation profiling of the use of metabolic pathways was done by the addition of oligomycin (1 μM), carbonyl cyanide-4-(trifluoromethoxy) phenylhydrazone (FCCP, 2 μM), and rotenone (1 μM; all are given as final concentrations, all from Sigma-Aldrich). For a description of how the various metabolic parameters were calculated, see fig. S1. The contribution of FAO to OCR was assessed by the addition of etomoxir (40 μM, Sigma-Aldrich). Assessment of the OCR of isolated mitochondria was also performed with the Seahorse $XF^e96$ metabolic extracellular flux analyzer and followed a protocol described previously (38). Sorted effector-memory $CD4^+$ T cells were plated onto Seahorse cell plates, as described earlier, in RPMI/10%AB containing TGF-β (5 ng/ml) where indicated in the figure legends and cultured at 37°C and 5%$CO_2$ for 5 hours. The medium was then exchanged for mannitol and sucrose (MAS) buffer [70 mM sucrose, 220 mM mannitol, 10 mM $KH_2PO_4$, 5 mM $MgCl_2$, 2 mM HEPES, 1 mM EGTA (pH 7.2), all reagents from Sigma-Aldrich] containing fatty acid–free bovine serum albumin (BSA, 4 mg/ml, Sigma-Aldrich). During the assay, first plasma membrane permeabilizer (PMP, 1 nM, Seahorse Bioscience) and then the following substrates (final concentrations given) together with ADP (1 mM) and FCCP (2 μM, both from Sigma-Aldrich) were added: Complex I: Pyruvate (5 mM)/Malate (2.5 mM, both from Sigma-Aldrich); Complex II: Succinate (10 mM, Sigma-Aldrich); Complex III: Duroquinol (0.5 mM, TCI America); Complex IV: tetramethyl-p-phenylenediamine (TMPD, 0.5 mM)/Ascorbate (2 mM, both from Sigma-Aldrich). Finally, the following specific inhibitors were added: Complex I: Rotenone (1 μM); Complex II: Malonate (40 μM); Complex III: Antimycin A (20 μM); Complex IV: Sodium Azide (20 mM, all from Sigma-Aldrich.)

**Flow cytometric analysis of protein abundance and phosphorylation**

Phosphorylation of Smad2/3 was assessed in cells ($0.2 \times 10^6$) previously fixed for 20 min at 37°C with fixation/permeabilization solution (BD Biosciences), permeabilized for 30 min at 4°C with Phosflow Perm Buffer III (BD Biosciences), and washed twice with phosphate-buffered saline (PBS) by staining for 30 min with Alexa Fluor 647–conjugated anti-pSmad2/3 (clone O72-670, BD Biosciences), further washing, and analysis. For assessment of IFN-γ production by intracellular cytokine staining, cells ($0.2 \times 10^6$) were re-stimulated for 16 hours with soluble anti-CD3 and anti-CD28 (1 and 5 μg/ml, respectively) in culture conditions as indicated in the figure legends, and then treated for 4 hours with PMA (10 ng/ml; Sigma-Aldrich) and ionomycin (500 ng/ml; Sigma-Aldrich). During the final 2 hours of activation, the cells were treated with monensin (BioLegend) to block cytokine secretion. The cells were then washed and fixed for 20 min at 37°C with fixation/permeabilization solution and washed with permeabilization buffer before being stained for 45 min phycoerythrin (PE)-conjugated anti-IFN-γ (clone B27, ImmunoTools), and then undergoing further washing and analysis. FoxP3 abundance was assessed in cells ($0.2 \times 10^6$) previously fixed for 20 min at 37°C in FoxP3 fixation/permeabilization solution (ebioscience) and washed with FoxP3 permeabilization buffer (ebioscience) by staining for 45 min with anti-human FoxP3-PE (clone PCH101, ebioscience), which was followed by further washing and analysis.

**Detection of apoptosis**

Annexin V staining was performed to identify apoptotic cells by flow cytometry. Staining was performed using annexin V binding buffer (BD Biosciences) and FTIC-conjugated annexin V (ImmunoTools).

**ΔΨm measurement**

MitoTracker staining was performed to assess differences in $\Delta\Psi m$. Cells ($0.2 \times 10^6$) were incubated in RPMI 1640/10% AB with 100 nM Mitotracker Green or MitoTracker Red (Invitrogen) for 20 min at 37°C and 5% CO2 before undergoing washing and analysis by flow cytometry. $\Delta\Psi m$ was calculated as follows: Mitotracker Red MFI / Mitotracker Green MFI.

**Quantification of mRNA**

The relative abundances of mRNAs of interested were quantified by real-time RT-PCR (qPCR). The mRNA was extracted with Qiagen spin columns (Qiagen) and cDNA was transcribed with the GoScript Reverse Transcription System (Promega) according to the manufacturer's instructions. SYBR green or Taqman primers (Applied Biosystems) were used for qPCR analysis. See Supplementary Table 2 for further details.

**Western blotting analysis**

Cell lysates for Western blotting analysis were prepared in RIPA buffer (ThermoFischer Scientific) and protein concentrations were determined with a BCA protein assay kit (ThermoFischer Scientific). Whole-cell lysates were resolved by 4 to 15% SDS-PAGE and were transferred onto nitrocellulose membranes. The membranes were then incubated with the Total OXPHOS Human WB Antibody Cocktail (abcam, ab110411). The membranes were then stained with the appropriate secondary antibody IRDye 800CW–conjugated goat polyclonal antibody to rabbit IgG (926-32211) and IRDye 800CW– or IRDye 680RD–conjugated goat polyclonal antibody to mouse IgG (926-68070); both from LI-COR). The Odyssey imaging system (LICOR) was used for band detection.

**Imaging flow cytometry**

MTR staining was performed as described earlier. Subsequently, cells ($0.5 \times 10^6$) were fixed and stained for pSmad2/3 as described earlier. Finally, cells were resuspended in PBS with 300 nM DAPI (Molecular Probes) to stain nuclei and analyzed using the Imagestream X imaging flow cytometer.

Nuclear and mitochondrial masks were defined based on regions of DAPI/MTR intensity, respectively, and colocalization was calculated using analysis tools in IDEAS software.

**Biochemical assays of ETC function**

Complex I (ab109721), II (ab109908), IV (ab109909) and V (ab109714) function was assessed in lysates from 5 to 10 x $10^6$ activated CD4$^+$ T cells using the indicated kits from Mitosciences (abcam) according to the manufacturer's instructions.

**Cytokine measurements in culture medium**

Cytokine production by T cells was measured using the Th1/Th2/Th17 Cytokine Bead Array (560484, BD Biosciences) or by ELISA for IFN-γ (ebiosciences) according to the manufacturers' instructions. The amount of IFN-γ present in total tumor-associated cell cultures was normalized (based on flow cytometry phenotyping) for 50,000 CD4$^+$ T cells.

**TGF-β ELISA**

TGF-β concentrations in cell culture medium were measured using the human TGF-β ELISA set (BD Biosciences), according to the manufacturer's instructions.

**Statistics**

Data were tested for normality with the Shapiro–Wilkins test. Data with normal distribution were assessed by paired Student two-sided t test. Multiple groups were compared by one- or two-way ANOVA, and a Bonferroni post-test for multiple comparisons. Non-normally distributed data were compared using a Wilcoxon test. Error bars represent SEM of the data presented.

**Study approval**

Blood samples were obtained from healthy donors after written informed consent. The study was approved by the Swiss Red Cross (blood transfusion service) and Institutional Review Board. Tumor

effusion fluids were collected from cancer patients presenting with malignant effusions at the University Hospital Basel after obtaining written informed consent.

**List of Supplementary Materials**

Supplementary Table 1

Supplementary Table 2

Supplementary Figure 1

Supplementary Figure 2

Supplementary Figure 3

Supplementary Figure 4

Supplementary Figure 5

Supplementary Figure 6

Supplementary Figure 7

Supplementary Figure 8

Supplementary Figure 9

Supplementary Figure 10

## References

1. L. Yang, Y. Pang, H. L. Moses, TGF-beta and immune cells: an important regulatory axis in the tumor microenvironment and progression, *Trends Immunol.* **31**, 220–227 (2010).

2. M. M. Shull, I. Ormsby, A. B. Kier, S. Pawlowski, R. J. Diebold, M. Yin, R. Allen, C. Sidman, G. Proetzel, D. Calvin, Targeted disruption of the mouse transforming growth factor-beta 1 gene results in multifocal inflammatory disease, *Nature* **359**, 693–699 (1992).

3. L. Gorelik, R. A. Flavell, Abrogation of TGFbeta signaling in T cells leads to spontaneous T cell differentiation and autoimmune disease, *Immunity* **12**, 171–181 (2000).

4. J. C. Marie, D. Liggitt, A. Y. Rudensky, Cellular mechanisms of fatal early-onset autoimmunity in mice with the T cell-specific targeting of transforming growth factor-beta receptor, *Immunity* **25**, 441–454 (2006).

5. M. O. Li, S. Sanjabi, R. A. Flavell, Transforming growth factor-beta controls development, homeostasis, and tolerance of T cells by regulatory T cell-dependent and -independent mechanisms, *Immunity* **25**, 455–471 (2006).

6. W. Ouyang, O. Beckett, Q. Ma, M. O. Li, Transforming growth factor-beta signaling curbs thymic negative selection promoting regulatory T cell development, *Immunity* **32**, 642–653 (2010).

7. Y. Liu, P. Zhang, J. Li, A. B. Kulkarni, S. Perruche, W. Chen, A critical function for TGF-beta signaling in the development of natural CD4+CD25+Foxp3+ regulatory T cells, *Nat. Immunol.* **9**, 632–640 (2008).

8. ClinicalTrials.gov (available at https://www.clinicaltrialsregister.eu).

9. M. A. Travis, D. Sheppard, TGF-β activation and function in immunity, *Annu Rev Immunol* **32**, 51–82 (2014).

10. A.-D. Gu, S. Zhang, Y. Wang, H. Xiong, T. A. Curtis, Y. Y. Wan, A Critical Role for Transcription Factor Smad4 in T Cell Function that Is Independent of Transforming Growth Factor β Receptor Signaling, *Immunity* **42**, 68–79 (2015).

11. E. Miyamoto-Sato, S. Fujimori, M. Ishizaka, N. Hirai, K. Masuoka, R. Saito, Y. Ozawa, K. Hino, T. Washio, M. Tomita, T. Yamashita, T. Oshikubo, H. Akasaka, J. Sugiyama, Y. Matsumoto, H. Yanagawa, J. Peccoud, Ed. A Comprehensive Resource of Interacting Protein Regions for Refining Human Transcription Factor Networks, *PLoS ONE* **5**, e9289–11 (2010).

12. L. Pang, T. Qiu, X. Cao, M. Wan, Apoptotic role of TGF-beta mediated by Smad4 mitochondria translocation and cytochrome c oxidase subunit II interaction, *Exp Cell Res* **317**, 1608–1620 (2011).

13. D. S. Thommen, J. Schreiner, P. Müller, P. Herzig, A. Roller, A. Belousov, P. Umana, P. Pisa, C. Klein, M. Bacac, O. S. Fischer, W. Moersig, S. Savic Prince, V. Levitsky, V. Karanikas, D. Lardinois, A. Zippelius, Progression of Lung Cancer Is Associated with Increased Dysfunction of T Cells Defined by Coexpression of Multiple Inhibitory Receptors, *Cancer Immunol Res* **3**, 1344–

1355 (2015).

14. G. J. Inman, F. J. Nicolás, J. F. Callahan, J. D. Harling, L. M. Gaster, A. D. Reith, N. J. Laping, C. S. Hill, SB-431542 is a potent and specific inhibitor of transforming growth factor-beta superfamily type I activin receptor-like kinase (ALK) receptors ALK4, ALK5, and ALK7, *Mol Pharmacol* **62**, 65–74 (2002).

15. K. M. Wagstaff, H. Sivakumaran, S. M. Heaton, D. Harrich, D. A. Jans, Ivermectin is a specific inhibitor of importin α/β-mediated nuclear import able to inhibit replication of HIV-1 and dengue virus, *Biochem J* **443**, 851–856 (2012).

16. Z. Xiao, X. Liu, H. F. Lodish, Importin beta mediates nuclear translocation of Smad 3, *J. Biol. Chem.* **275**, 23425–23428 (2000).

17. R. D. Michalek, V. A. Gerriets, S. R. Jacobs, A. N. Macintyre, N. J. MacIver, E. F. Mason, S. A. Sullivan, A. G. Nichols, J. C. Rathmell, Cutting edge: distinct glycolytic and lipid oxidative metabolic programs are essential for effector and regulatory CD4+ T cell subsets, *J. Immunol.* **186**, 3299–3303 (2011).

18. M. Jüllig, N. S. Stott, Mitochondrial localization of Smad5 in a human chondrogenic cell line, *Biochem. Biophys. Res. Commun.* **307**, 108–113 (2003).

19. E. L. Pearce, M. C. Poffenberger, C.-H. Chang, R. G. Jones, Fueling immunity: insights into metabolism and lymphocyte function, *Science* **342**, 1242454 (2013).

20. J. T. Lin, S. L. Martin, L. Xia, J. D. Gorham, TGF-beta 1 uses distinct mechanisms to inhibit IFN-gamma expression in CD4+ T cells at priming and at recall: differential involvement of Stat4 and T-bet, *J. Immunol.* **174**, 5950–5958 (2005).

21. M. J. Dobrzanski, Expanding roles for CD4 T cells and their subpopulations in tumor immunity and therapy, *Front Oncol* **3**, 63 (2013).

22. J. Yan, H. Zhang, Y. Yin, J. Li, Y. Tang, S. Purkayastha, L. Li, D. Cai, Obesity- and aging-induced excess of central transforming growth factor-β potentiates diabetic development via an RNA stress response, *Nat. Med.* **20**, 1001–1008 (2014).

23. H. Yadav, C. Quijano, A. K. Kamaraju, O. Gavrilova, R. Malek, W. Chen, P. Zerfas, D. Zhigang, E. C. Wright, C. Stuelten, P. Sun, S. Lonning, M. Skarulis, A. E. Sumner, T. Finkel, S. G. Rane, Protection from obesity and diabetes by blockade of TGF-beta/Smad3 signaling, *Cell Metab.* **14**, 67–79 (2011).

24. U. I. Heine, J. K. Burmester, K. C. Flanders, D. Danielpour, E. F. Munoz, A. B. Roberts, M. B. Sporn, Localization of transforming growth factor-beta 1 in mitochondria of murine heart and liver, *Cell Regul.* **2**, 467–477 (1991).

25. S. Roth-Eichhorn, K. Kühl, A. M. Gressner, Subcellular localization of (latent) transforming growth factor beta and the latent TGF-beta binding protein in rat hepatocytes and hepatic stellate cells, *Hepatology* **28**, 1588–1596 (1998).

26. W. Chen, W. Jin, H. Tian, P. Sicurello, M. Frank, J. M. Orenstein, S. M. Wahl, Requirement for transforming growth factor beta1 in controlling T cell apoptosis, *J. Exp. Med.* **194**, 439–453 (2001).

27. C. Guido, D. Whitaker-Menezes, C. Capparelli, R. Balliet, Z. Lin, R. G. Pestell, A. Howell, S. Aquila, S. Ando, U. Martinez-Outschoorn, F. Sotgia, M. P. Lisanti, Metabolic reprogramming of cancer-associated fibroblasts by TGF-beta drives tumor growth: connecting TGF-beta signaling with "Warburg-like" cancer metabolism and L-lactate production, *Cell Cycle* **11**, 3019–3035 (2012).

28. Y.-S. Yoon, J.-H. Lee, S.-C. Hwang, K. S. Choi, G. Yoon, TGF beta1 induces prolonged mitochondrial ROS generation through decreased complex IV activity with senescent arrest in Mv1Lu cells, *Oncogene* **24**, 1895–1903 (2005).

29. H.-O. Byun, H.-J. Jung, Y.-H. Seo, Y.-K. Lee, S.-C. Hwang, E. Seong Hwang, G. Yoon, GSK3 inactivation is involved in mitochondrial complex IV defect in transforming growth factor (TGF) β1-induced senescence, *Exp Cell Res* **318**, 1808–1819 (2012).

30. N. Stieger, K. Worthmann, B. Teng, S. Engeli, A. M. Das, H. Haller, M. Schiffer, Impact of high glucose and transforming growth factor-beta on bioenergetic profiles in podocytes, *Metabolism* **61**, 1073–1086 (2012).

31. P. Pacher, K. Sharma, G. Csordas, Y. Zhu, G. Hajnoczky, Uncoupling of ER-mitochondrial calcium communication by transforming growth factor-beta, *Am J Physiol Renal Physiol* **295**, F1303–12 (2008).

32. P. M. Gubser, G. R. Bantug, L. Razik, M. Fischer, S. Dimeloe, G. Hoenger, B. Durovic, A. Jauch, C. Hess, Rapid effector function of memory CD8(+) T cells requires an immediate-early glycolytic switch, *Nat. Immunol.* **14**, 1064–1072 (2013).

33. C.-H. Chang, J. D. Curtis, L. B. Maggi, B. Faubert, A. V. Villarino, D. O Sullivan, S. C.-C. Huang, G. J. W. van der Windt, J. Blagih, J. Qiu, J. D. Weber, E. J. Pearce, R. G. Jones, E. L. Pearce, Posttranscriptional Control of T Cell Effector Function by Aerobic Glycolysis*Cell* **153**, 1239–1251 (2013).

34. N. Patsoukis, K. Bardhan, P. Chatterjee, D. Sari, B. Liu, L. N. Bell, E. D. Karoly, G. J. Freeman, V. Petkova, P. Seth, L. Li, V. A. Boussiotis, PD-1 alters T-cell metabolic reprogramming by inhibiting glycolysis and promoting lipolysis and fatty acid oxidation, *Nat Commun* **6**, 6692 (2015).

35. C.-H. Chang, J. Qiu, D. O'Sullivan, M. D. Buck, T. Noguchi, J. D. Curtis, Q. Chen, M. Gindin, M. M. Gubin, G. J. W. van der Windt, E. Tonc, R. D. Schreiber, E. J. Pearce, E. L. Pearce, Metabolic Competition in the Tumor Microenvironment Is a Driver of Cancer Progression, *Cell* **162**, 1229–1241 (2015).

36. P.-C. Ho, J. D. Bihuniak, A. N. Macintyre, M. Staron, X. Liu, R. Amezquita, Y.-C. Tsui, G. Cui, G. Micevic, J. C. Perales, S. H. Kleinstein, E. D. Abel, K. L. Insogna, S. Feske, J. W. Locasale, M. W. Bosenberg, J. C. Rathmell, S. M. Kaech, Phosphoenolpyruvate Is a Metabolic Checkpoint of Anti-tumor T Cell Responses, *Cell* **162**, 1217–1228 (2015).

37. S. Dimeloe, C. Frick, M. Fischer, P. M. Gubser, L. Razik, G. R. Bantug, M. Ravon, A. Langenkamp, C. Hess, Human regulatory T cells lack the cyclophosphamide-extruding transporter ABCB1 and are more susceptible to cyclophosphamide-induced apoptosis, *Eur. J. Immunol.* **44**, 3614–3620 (2014).

38. J. K. Salabei, A. A. Gibb, B. G. Hill, Comprehensive measurement of respiratory activity in permeabilized cells using extracellular flux analysis, Nat Protoc 9, 421–438 (2014).

**Author Contributions**

S.D. designed, performed and analyzed most experiments, and wrote the manuscript; J.L., C.F., L.D., M.F., F.M, G.R.B. and Y.L. performed experiments; D.T and A.Z. obtained and prepared tumor effusion samples and provided intellectual input regarding experimental design and interpretation; A.L and C.H. oversaw the study and experiments and C.H. wrote the manuscript.

**Competing interests**

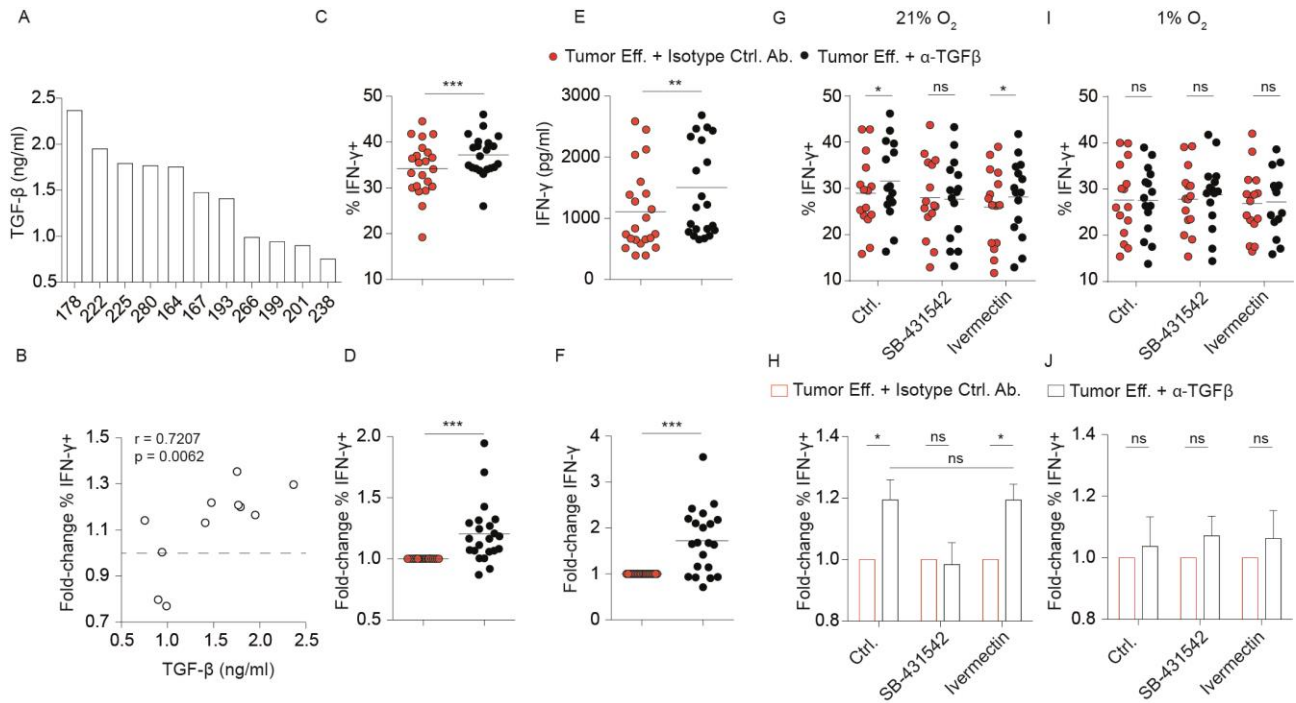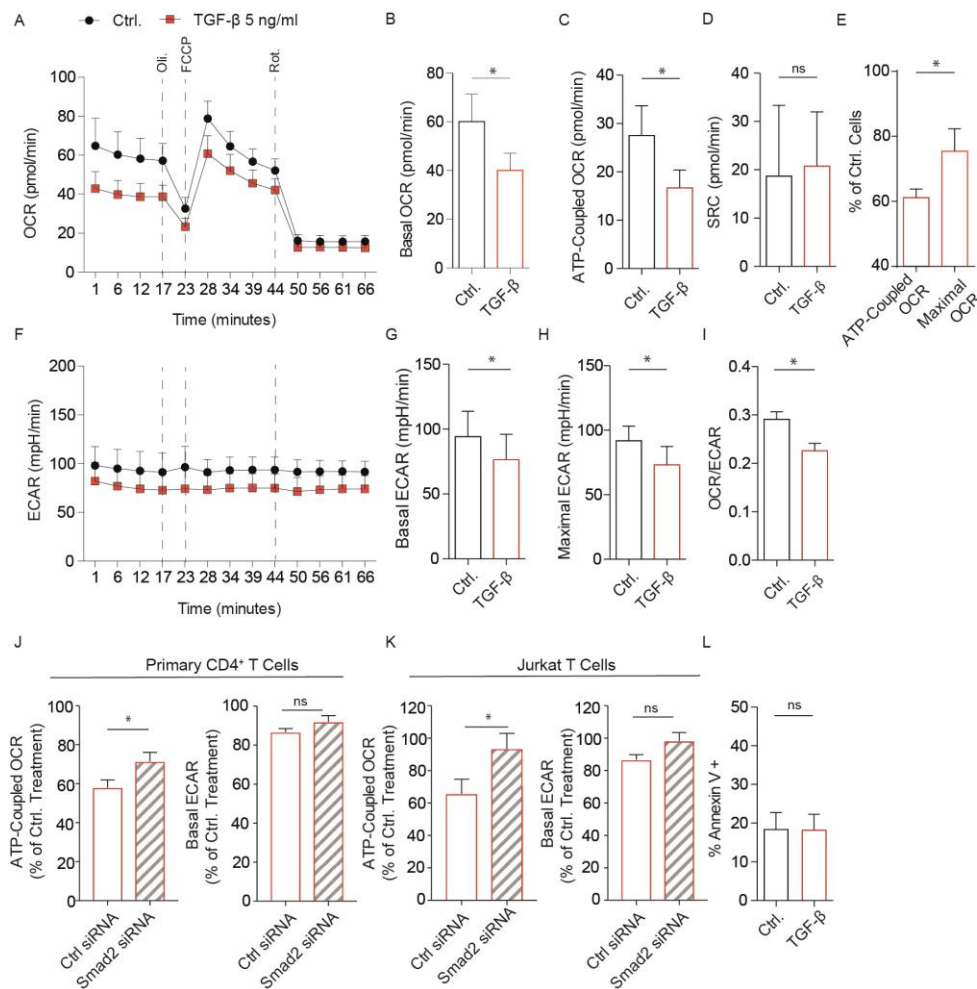The authors declare that they have no competing interests.

**Figure 1: Tumor-derived TGF-β inhibits EM CD4$^+$ T cell IFN-γ production, requiring Smad phosphorylation but not nuclear translocation**

(A) Quantification of TGF-β levels in 11 tumor effusions (see **Supplementary Table 1** for patient details). (B-F) Activated EM CD4$^+$ T cells were restimulated for 16 hours in tumor supernatant (50% with 50% serum-free medium) with additionally either an isotype control antibody or TGF-β neutralizing mAb. (B) For each tumor effusion, comparisons were made of mean fold change in IFN-γ positive (+) cells (α-TGF-β / isotype control mAb) as assessed by flow cytometry, corrected for dilution (factor 2) of tumor effusion fluid, with the concentration of TGF-β present in the sample (as described in **Figure 1A/Supplementary Table 1**) (n=11 pairs, each effusion tested on 3-5 independent healthy donors), (C) percentage of IFN-γ producing (+) cells and (D) corrected fold increase of IFN-γ producing (+) cells; (E) abundance and (F) corrected fold change of IFN-γ secreted into the supernatant (C-F n=22, combined data for 8 tumor effusions (178, 222, 225, 280, 238, 164, 193, 167), each tested on 3-6 independent donors). (G) percentage of IFN-γ producing (+) cells and

(H) Corrected fold change in IFN-$\gamma$ positive (+) cells ($\alpha$-TGF-$\beta$ / isotype control mAb) among activated EM CD4$^+$ T cells, pre-treated for 30 min. with SB-431542 (10 µM) or ivermectin (5 µM) as indicated, then re-stimulated for 16 hours in presence of tumor effusion as described, plus isotype control (red dots/bars) or $\alpha$-TGF-$\beta$ mAb (black dots/bars) at 21% oxygen (I,J) as for (G,H) but performed at 1% oxygen. Tumor effusions 178, 222, 225 and 167 were used (n = 14/15, at least n=3 independent donors for each effusion). p values were calculated by: (B) Pearson correlation; (C,E) paired t test; (D,F) Wilcoxon test; (G-J) two-way ANOVA. *p<0.05, **p<0.01 ***p<0.0001.

**Figure 2: TGF-β diminishes respiratory capacity of activated EM CD4⁺ T cells**

(A) OCR profile, (B) basal OCR, (C) ATP-coupled OCR, (D) SRC and (E) % of control ATP-Coupled and Maximal OCR; (F) ECAR, (G) basal and (H) maximal ECAR of activated EM CD4⁺ T cells, treated for 16 hours with either control medium (black line) or TGF-β (5 ng/ml, red line) as indicated, then assessed for metabolic parameters as described in **Supplementary Figure 2** (n=4 independent donors). (I) ATP-coupled OCR/basal ECAR (OCR/ECAR) ratio of activated EM CD4⁺ T cells treated as in (A-F) (n=4 independent donors). (J-K) ATP-coupled OCR and basal ECAR of (J) total primary CD4⁺ T cells (n=9 independent donors) or (K) Jurkat T cells (n=3 biological replicates), transfected with Smad2 or control scrambled siRNA and then treated with TGF-β-treated as in (A-I) (expressed as a percentage of rates under control treatment in absence of TGF-β). (L)

Percentage of Annexin V positive (+) cells amongst activated EM CD4$^+$ T cells treated as in (A-F)

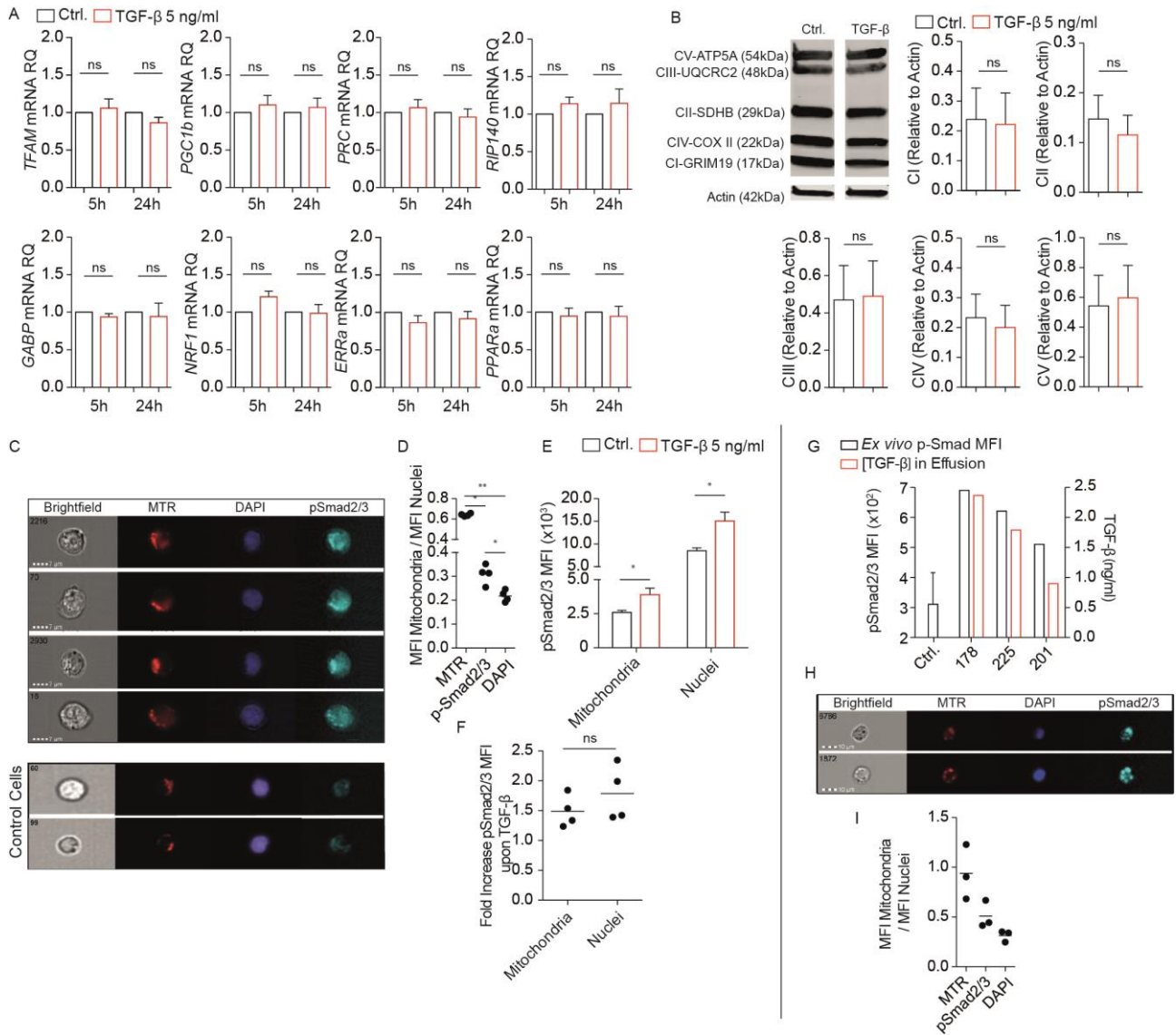(n=5 independent donors). All p values were calculated by paired t test. *p<0.05.

**Figure 3: Smad proteins are present in mitochondria of CD4+ T cells**

(A) mRNA levels in activated, total CD4+ T cells, quantified relative to ribosomal 18s RNA and expressed as relative quantities (RQ) compared to control treatment for the genes indicated, under control treatment (Ctrl., black bars) or TGF-β treatment (5 ng/ml, red bars) for 5 or 24 hours as indicated (n=6 independent donors). (B) Example Western Blot (non-contiguous lanes) and summary data (expressed relative to actin abundance) for mitochondrial electron transport chain (ETC) complex I-V protein expression in activated, total CD4+ T cells, under control treatment (Ctrl., black bars) or TGF-β treatment (5 ng/ml, red bars) for 24 hours (n=5 independent donors). ml(C) Example

images of activated, total control (lower) CD4$^+$ T cells or cells treated with TGF-β (5 ng/ml) for 1 hour (upper), then stained with mitotracker red (MTR, red), DAPI (blue) and anti-pSmad2/3 (turquoise), and analyzed using Imagestream X. (D) Summary data of mean fluorescence intensity (MFI) in mitochondria / MFI in nuclei of the fluorochromes indicated, in total CD4$^+$ T cells treated with TGF-β as in (F) (n=4 independent donors, MFIs of >2000 cells per condition and per donor). (E) Summary data of pSmad2/3 mean fluorescence intensity (MFI) on defined mitochondrial and nuclear regions in control (Ctrl., black bars) and TGF-β-treated (5 ng/ml, red bars) CD4$^+$ T cells (n=4 independent donors). (F) Fold increase in pSmad2/3 MFI in mitochondrial and nuclear regions of total CD4$^+$ T cells treated as in (E) (n=4 independent donors). (G) pSmad2/3 MFI assessed by flow cytometry (black bars, left y axis) of tumor-associated CD4$^+$ T cells (from effusions 178, 225 and 201) stained ex vivo, compared with effusion TGF-β concentration (red bars, right y axis). (H) Example images (from sample 201) of CD4$^+$ T cells (gated on CD4) among tumor-associated cells, stained ex vivo with mitotracker red (MTR, red), DAPI (blue) and anti-pSmad2/3 (turquoise), and analyzed using Imagestream X. (I) Summary data of (MFI) in mitochondria / MFI in nuclei in cells treated as in (H) (n=3 independent donors, MFIs of >2000 cells per donor). p values were calculated by: (A) Wilcoxon test, (B,F) paired t test, (D) one-way ANOVA, (E) two-way ANOVA. *p<0.05 **p<0.01.
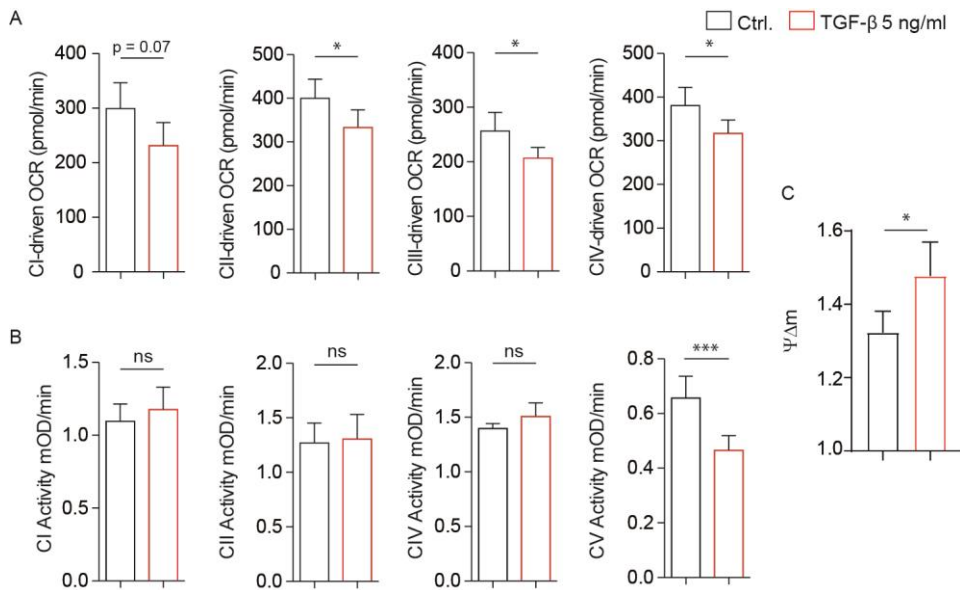
**Figure 4: TGF-β specifically inhibits activity of ATP-Synthase**

(A) Mean OCR of activated, EM CD4+ T cells treated for 5 hours either with control medium (Ctrl., black bars) or TGF-β (5 ng/ml, red bars), then permeabilized to assess mitochondrial respiration of specific substrates or in response to electron donors provided for complex I, II, III and IV (n=8 independent donors). (B) Mean activity of complexes I, II, IV and V as assessed by biochemical assay in activated, total CD4+ T cells treated for 5 hours either with control medium (Ctrl., black bars) or TGF-β (5 ng/ml, red bars) (n=10 independent donors). (C) Mitochondrial membrane potential (ΔΨm) of activated, total CD4+ T cells, expressed as a ratio of Mitospy Orange Mean Fluorescence Intensity in untreated vs. FCCP-treated cells previously treated with control medium or TGF-β as in (B) (n=4 independent donors). p values were calculated by: (A) Wilcoxon test; (B,C) paired t test;. *p<0.05, ***p<0.0001.
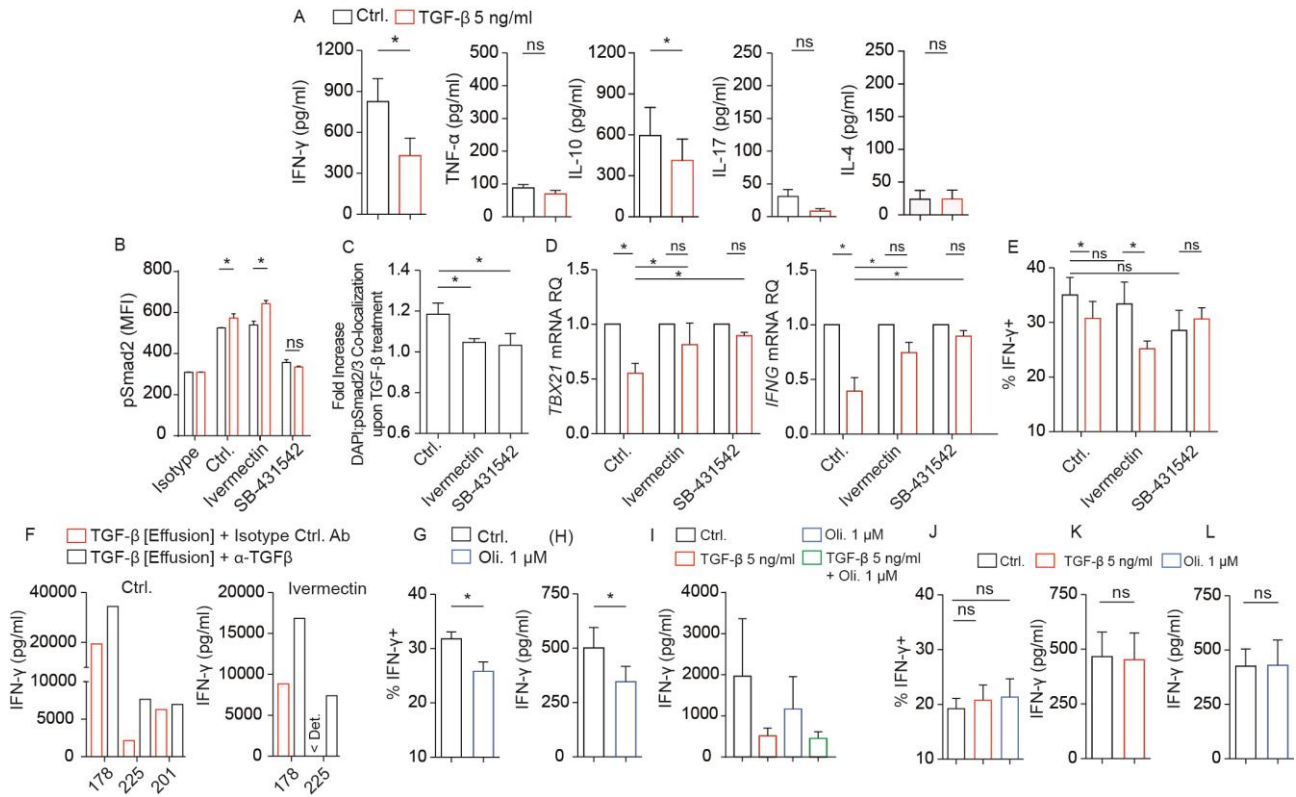
**Figure 5: TGF-β inhibits EM CD4⁺ T cell IFN-γ expression independently of nuclear Smad import, but depending on mitochondrial respiration**

(A) IFN-γ, TNF-α, IL-10, IL-17A and IL-4 secreted by activated EM CD4⁺ T cells restimulated for 16 hours in control medium (Ctrl., black bars) or treated with TGF-β (5 ng/ml, red bars), and measured from supernatant by CBA (n=6 independent donors). (B) MFI of isotype control antibody staining or anti-pSmad2/3 antibody staining in activated, total CD4⁺ T cells, pre-treated with ivermectin (5 μM) or SB-431542 (10 μM) for 30 min., then treated for 1 hour with control medium (black bars) or TGF-β (5 ng/ml red bars) (n=3 independent donors). (C) Fold increase in colocalization of fluorescence between DAPI (nuclear marker) and pSmad2/3 in cells treated as in (B) (n=4 independent donors). (D) mRNA levels, quantified relative to ribosomal 18s RNA and expressed as relative quantities (RQ), compared to control treatment for TBX21 or IFNG in total, activated CD4⁺ T cells, pre-treated for 30 min. with ivermectin or SB-431542 as indicated then cultured for 16 hours, with either control

36

medium (Ctrl., black bars) or TGF-β (5 ng/ml, red bars) (n=3 independent donors). (E) Percentage IFN-γ positive (+) cells among activated EM CD4$^+$ T cells pre-treated for 30 min. with ivermectin or SB-431542 as indicated, then re-stimulated overnight in the presence of control medium (Ctrl., black bars) or TGF-β (5 ng/ml, red bars) (n=5 independent donors). (F) IFN-γ content of supernatants from tumor-associated cells, stimulated overnight with anti-CD3/anti-CD28 mAb in the presence of TGF-β (level as per effusion, see **Fig. 1A** and **Tbl. 1**), plus additionally either an isotype control antibody (red bars) or TGF-β neutralizing mAb (black bars), performed either in control conditions (right panel, n=3 independent donors) on in presence of ivermectin (5 μM, left panel, n=2 independent donors, < Det. = below assay detection limit). (G) Percentage IFN-γ producing (+) cells among activated EM CD4$^+$ T cells restimulated for 16 hours in control medium (Ctrl., black bar) or in presence of Oligomycin (1 μM, blue bar) (n=5 independent donors). (H) IFN-γ measured from cell culture supernatants of EM CD4$^+$ T cells, treated as in (H) (n=8 independent donors). (I) IFN-γ measured from cell culture supernatants of EM CD4$^+$ T cells restimulated for 16 hours in control medium or in presence of TGF-β and/or Oligomycin as indicated (n=4 independent donors) (J) Percentage of IFN-γ producing (+) cells among activated EM CD4$^+$ T cells restimulated for 16 hours at 1% atmospheric oxygen in control medium (Ctrl., black bar) or in presence of TGF-β (5 ng/ml, red bar) or Oligomycin (1 μM, blue bar) (n=5 independent donors). (K,L) IFN-γ measured from cell culture supernatants of EM CD4$^+$ T cells, treated as in (J) (n=6-8 independent donors). p values calculated by (A,H,I,K,L) paired t test, (B,D,E,F) two-way ANOVA, (C,J) one-way ANOVA. *p<0.05.
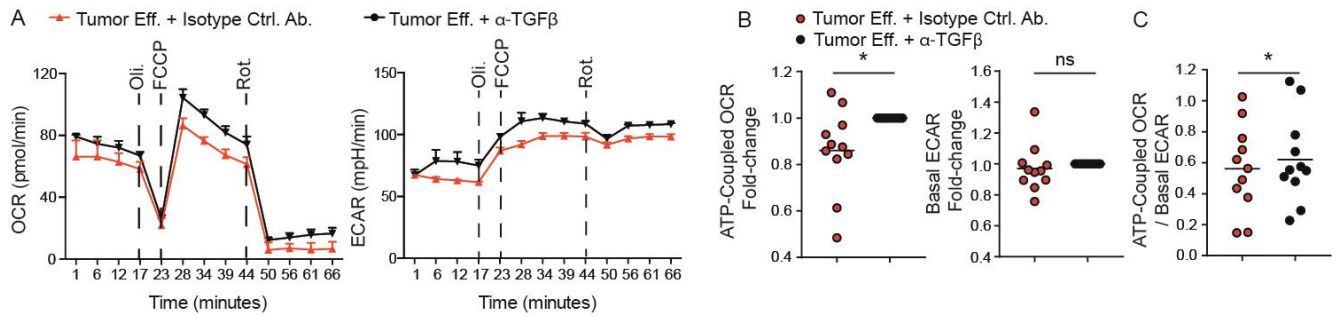
**Figure 6: Tumor-derived TGF-β inhibits EM CD4$^+$ T cell metabolism**

(A) OCR and ECAR of activated EM CD4$^+$ T cells pre-incubated for 5 hours in tumor supernatant (50% with 50% serum-free medium) with additionally either an isotype control antibody (red line), or TGF-β neutralizing mAb (α-TGF-β, black line), additionally treated with Oligomycin (Oli. 1μM), FCCP (2 μM) and Rotenone (1 μM) as indicated to measure metabolic parameters as described in **Supplementary Figure 1** (representative example with effusion 178). (B) Fold change in ATP-coupled OCR and basal ECAR in cells treated as in (A), isotype control antibody (red circles) TGF-β neutralizing mAb (α-TGF-β, black circles) (n=7 independent donors, combined data for experiments with effusion 178 and 225). (C) ATP-coupled OCR/basal ECAR ratios of cells treated as in (A). p values were calculated by (B) Wilcoxon Test (C) paired t test. *$p < 0.05$